Original Article

CircHSPG2 absence weakens hypoxia-induced dysfunction in cardiomyocytes by targeting the miR-25-3p/PAWR axis

Ying Zhao[1], Shujun Wang[1], Shufang Liu[2], Qingfeng Yan[3], Yueping Li[4], Yunzhong Liu[1]

[1]The Department of Cardio and Thoracic Surgery, The First Affiliated Hospital of Hainan Medical University, Haikou, China; [2]The Department of Hematology, The First Affiliated Hospital of Hainan Medical University, Haikou, China; [3]The Department of Pathophysiology, Hainan Medical College, Haikou, China; [4]The Department of Histology and Embryology, Hainan Medical College, Haikou, China

Contributions: (I) Conception and design: Y Liu; (II) Administrative support: None; (III) Provision of study materials: Y Zhao, S Wang; (IV) Collection and assembly of data: S Liu, Q Yan; (V) Data analysis and interpretation: S Liu, Q Yan; (VI) Manuscript writing: All authors; (VII) Final approval of manuscript: All authors.

Correspondence to: Yunzhong Liu. The Department of Cardio and Thoracic Surgery, The First Affiliated Hospital of Hainan Medical University, No. 31, Longhua Road, Haikou 570102, China. Email: lyzhaaaa@163.com.

Background: Circular RNAs (circRNAs) are important regulators in human cardiovascular diseases. Here, we investigated the role of circRNA heparan sulfate proteoglycan 2 (circHSPG2) in hypoxia-induced myocardial infarction (MI) and its associated mechanism.

Methods: Reverse transcription-quantitative polymerase chain reaction (RT-qPCR) and Western blot assay were conducted to examine RNA and protein expression. Cell viability was analyzed by 3-(4,5-Dimethylthiazol-2-yl)-2,5-Diphenyltetrazolium Bromide (MTT) assay. Cell proliferation was assessed by 5-Ethynyl-2'-deoxyuridine (EdU) assay and colony formation assay. Flow cytometry (FCM) analysis was carried out to analyze the apoptosis of AC-16 cells. Lactate dehydrogenase (LDH) assay was implemented to assess cell death. Dual-luciferase reporter assay and RNA immunoprecipitation (RIP) assay were performed to verify the target relationship between microRNA-25-3p (miR-25-3p) and circHSPG2 or pro-apoptotic WT1 regulator (PAWR).

Results: Hypoxia treatment up-regulated the expression of circHSPG2 in AC-16 cells. Hypoxia exposure reduced the viability, suppressed the proliferation and induced the apoptosis of AC-16 cells, and these effects were diminished by the silence of circHSPG2. CircHSPG2 acted as a molecular sponge for miR-25-3p. CircHSPG2 absence-mediated effects on hypoxia-induced AC-16 cells were largely reversed by anti-miR-25-3p. miR-25-3p bound to the 3' untranslated region (3'UTR) of PAWR. PAWR overexpression largely counteracted miR-25-3p-mediated effects on hypoxia-induced AC-16 cells. CircHSPG2 positively regulated the expression of PAWR by acting as miR-25-3p sponge in AC-16 cells.

Conclusions: CircHSPG2 silencing protected AC-16 cells against hypoxia-induced dysfunction by targeting miR-25-3p/PAWR axis.

Keywords: Myocardial infarction (MI); hypoxia; circHSPG2; miR-25-3p; pro-apoptotic WT1 regulator (PAWR)

Submitted Apr 20, 2022. Accepted for publication Sep 05, 2022.
doi: 10.21037/cdt-22-197
View this article at: https://dx.doi.org/10.21037/cdt-22-197

Introduction

Myocardial infarction (MI) is one of the leading pathological causes of disability and mortality in cardiovascular diseases (1). The apoptosis, hypertrophy, and inflammatory response of cardiomyocytes are related to MI (2,3), which eventually results in heart failure (4,5). Cardiomyocytes are terminally differentiated cells without regenerative potential. Therefore, investigating the molecular mechanism behind hypoxia-induced dysfunction of cardiomyocytes is essential to improve the clinical treatment strategies for MI.

Circular RNAs (circRNAs) are implicated in the regulation of almost all cellular processes, and previous articles have pointed out that circRNAs play pivotal functions in the pathogenesis of multiple heart diseases, including MI, heart failure, and hypertrophy (6,7). CircRNA heparan sulfate proteoglycan 2 (circHSPG2; hsa_circ_0010729) is a newly discovered circRNA, which is related to hypoxia-induced growth of vascular endothelial cells (8). Lei *et al*. found that circHSPG2 silencing attenuates hypoxia-induced cardiomyocyte injuries by releasing miR-27a-3p and repressing *TRAF5* expression (9). Moreover, Zhang *et al*. demonstrated that hypoxia exposure enhances circHSPG2 expression in cardiomyocytes, and circHSPG2 silencing suppresses hypoxia-evoked injury in cardiomyocytes through mediating miR-370-3p/*TRAF6* signaling cascade (10). The potential regulatory mechanism behind the protective role of circHSPG2 in hypoxia-induced cardiomyocytes was further explored.

Accumulating evidence has demonstrated that circRNAs can regulate cell biological behaviors by acting as microRNA (miRNA) sponges (11). miRNAs play pivotal regulatory roles in cardiovascular diseases, including dilated cardiomyopathy (12), cardiac remodeling (13), and heart failure (14). Through bioinformatics analysis via Starbase database, it was found that miR-25-3p harbored the complementary sites with circHSPG2. Pan *et al*. demonstrated that miR-25 overexpression protects cardiomyocytes from oxidation-mediated injury by regulating mitochondrial calcium uniporter expression (15). Yao *et al*. found that miR-25 attenuates sepsis-evoked apoptosis of cardiomyocytes by targeting *PTEN* (16). Qin *et al*. found that miR-25 abundance is reduced in hypoxia-induced cardiomyocytes, and it facilitates cell proliferation and migration abilities and hampers cell apoptosis in cardiomyocytes by modulating Bim (17). Here, the function of miR-25-3p and its related mechanism in hypoxia-induced myocardial damage were investigated in this study.

Through bioinformatics analysis using Starbase database, it was found that pro-apoptotic WT1 regulator (*PAWR*) possessed the complementary sites with miR-25-3p. Chai *et al*. found that *PAWR* expression is up-regulated in hypoxia-induced cardiomyocytes, and circ_0068655 facilitates the apoptosis of cardiomyocytes by up-regulating *PAWR* via sponging miR-498 (18). The associated relationship of miR-25-3p and PAWR was tested.

In the current study, we first analyzed the role of circHSPG2 in MI using hypoxia-induced AC-16 cell model. Then, bioinformatics analysis was conducted to establish circHSPG2/miRNA/mRNA axis, and rescue experiments were conducted to verify the working mechanism of circHSPG2 in hypoxia-induced AC-16 cells. We aimed to identify novel targets for MI intervention and treatment.

Methods

Cell culture

Human ventricular cardiomyocytes (AC-16) (19) were purchased from Beijing Institute for Cancer Research Collection (Beijing, China). Dulbecco's modified Eagle's medium/F12 (#11320033; DMEM/F12; Invitrogen, Waltham, MA, USA) with the supplement of 10% fetal bovine serum (#10099141C; FBS, Gibco, Carlsbad, CA, USA) and 1% penicillin/streptomycin solution (#15070063; Gibco) was utilized for the cultivation of AC-16 cells. AC-16 cells were cultured under the standard condition (5% CO_2, 37 ℃). The study was conducted in accordance with the Declaration of Helsinki (as revised in 2013).

Hypoxia treatment

AC-16 cells were cultured under the condition of 1% O_2, 94% N_2, and 5% CO_2 for 24 h to induce hypoxia, and cells growing under normoxic condition were regarded as the control.

Reverse transcription-quantitative polymerase chain reaction (RT-qPCR)

RNA samples were isolated from AC-16 cells using TRIzol reagent (#12183555; Invitrogen). The concentration and purity of RNA samples were analyzed using NanoDrop 2000 (NanoDrop Technologies, Wilmington, DE, USA). For circRNAs and mRNAs, reverse transcription was implemented using a commercial Prime-script RT reagent Kit (#RR037A; Takara, Dalian, China), and qPCR was carried out using a commercial Premix Ex Taq Kit (#RR047A; Takara). For miRNAs, complementary DNA (cDNA) was synthesized using a commercial Taqman MicroRNA Reverse Transcription Kit (#4366596; Applied Biosystems, Foster City, CA, USA), and thermal cycling reaction was carried out using a commercial Taqman Universal Master Mix II (#4440043; Applied Biosystems). qPCR reaction was conducted on 7500 Fast Real-Time PCR system (Thermo Fisher Scientific, Waltham, MA, USA). The thermo cycling condition was listed as below:

Table 1 Primer sequences in RT-qPCR assay

Gene	Sequence (5'-3')
circHSPG2	Forward: ATGCTGGGGTCTACATTTGC
	Reverse: ACTCGTAGCGCACGTTGTAA
HSPG2	Forward: CTCGTCCCACAACGAGCAG
	Reverse: GGTCGACTAGCTGGAACTCG
miR-25-3p	Forward: GCCGAGCATTGCACTTGTCT
	Reverse: CAGTGCAGGGTCCGAGGTAT
PAWR	Forward: CGTCGGGGTCCGTACTGTAG
	Reverse: TCGCCATATTCCCAAAGGGG
GAPDH	Forward: TATGATGACATCAAGAAGGTGGT
	Reverse: TGTAGCCAAATTCGTTGTCATAC
U6	Forward: GCTTCGGCAGCACATATACTAAAAT
	Reverse: CGCTTCACGAATTTGCGTGTCAT

RT-qPCR, reverse transcription-quantitative polymerase chain reaction.

95 ℃ for 3 min and 38 cycles of 95 ℃ for 20 sec, 60 ℃ for 30 sec, and 72 ℃ for 30 sec. All primers used in RT-qPCR were shown in *Table 1*. The relative fold changes were analyzed by the $2^{-\Delta\Delta Ct}$ method. RT-qPCR was repeated three times with three technical repetitions each time.

RNase R treatment and subcellular localization

The circular structure of circHSPG2 was tested with RNase R (Applied Biological Materials, Vancouver, Canada). RNA samples were treated with RNase R (100 μg/mL) at 37 ℃ for 20 min. RT-qPCR was implemented to analyze circHSPG2 and linear HSPG2 mRNA abundance. RT-qPCR was repeated three times with three technical repetitions each time.

The cytoplasmic and nuclear fractions of cicHSPG2 were isolated using the commercial PARIS^{TM} Kit (#AM1921; Thermo Fisher Scientific). This experiment was repeated three times.

Cell transfection

Small interfering (si)RNA against circHSPG2 (si-circHSPG2), negative control of siRNA (si-NC), overexpression plasmid of circHSPG2 (oe-circHSPG2), pLO-ciR vector (vector), mimics of miR-25-3p (miR-25-3p), miR-NC, inhibitor of miR-25-3p (anti-miR-25-3p), anti-miR-NC, PAWR overexpression plasmid (PAWR), and pcDNA3.1(+) were synthesized or constructed by Geneseed (Guangzhou, China) and GeneChem (Shanghai, China). Plasmid (1 μg), miRNA mimics (50 nM), or miRNA inhibitor (20 nM) was transfected into AC-16 cells using Lipofectamine 3000 (Invitrogen). For hypoxia and transfection co-treatment, AC-16 cells were induced by hypoxia for 24 h after transfection for 24 h.

3-(4,5-Dimethylthiazol-2-yl)-2,5-Diphenyltetrazolium Bromide (MTT) assay

A total of 5×10^3 AC-16 cells were seeded onto 96-well plates. The next day, AC-16 cells were incubated with 20 μL of MTT reagent (#11465007001; 5 mg/mL; Sigma, St. Louis, MO, USA) for 4 h at 37 ℃. Then, 100 μL of dimethyl sulfoxide (#11465007001; DMSO, Sigma) was pipetted to the wells to dissolve the formazan products, and the plates were gently shaken for 10 min. The optical density was examined at the wavelength of 570 nm under a microplate reader (Bio-Rad). MTT assay was repeated three times with six technical repetitions each time.

5-Ethynyl-2'-deoxyuridine (EdU) assay

AC-16 cells in 96-well plates were incubated with 50 μM EdU (#C10310-1; RiboBio, Guangzhou, China) for 1 h followed by immobilization with 100 μL of 4% paraformaldehyde (Sangon Biotech, Shanghai, China) at 25 ℃ for 30 min. Cell nucleus was marked with 100 ng/mL 4', 6-diamidino-2-phenylindole (#MBD0015; DAPI; Sigma) for 10 min. Five random fields were captured under a Nikon fluorescence microscope (Eclipse Ti2-U; Nikon) and the positive rate was analyzed. EdU assay was repeated three times with three technical repetitions each time.

Colony formation assay

AC-16 cells were seeded onto 12-well plates at 200 cells/well and were continued to culture for 12 d. The culture supernatant was replenished every 4 d. The colonies were immobilized with 4% paraformaldehyde (#E672002-0500; Sangon Biotech) for 15 min at room temperature, and were then stained with 0.5% crystal violet for 10 min at room temperature. Colony number (with more than 50 cells) was analyzed under an optical microscope (Olympus, Tokyo, Japan). Colony formation assay was repeated three times with three technical repetitions each time.

Flow cytometry (FCM) analysis

Cell apoptosis was analyzed by fluorescein isothiocyanate (FITC) and propidium iodide (PI) double-staining using the commercial Apoptosis Detection Kit (#40302ES20; Qcbio Science & Technologies, Shanghai, China). AC-16 cells were dispersed in 100 μL of binding buffer, and then cells were incubated with 10 μL of Annexin V-FITC and 10 μL of PI for 15 min at room temperature in the dark. Cells were loaded onto the flow cytometer (Beckman Coulter, Fullerton, CA, USA) for the analysis of apoptosis rate. FCM analysis was repeated three times with three technical repetitions each time.

Western blot assay

Proteins in AC-16 cells were isolated with the radioimmunoprecipitation assay (RIPA) lysis buffer (Sigma). Protein samples (35 μg) were loaded onto 10% separating gel and blotted onto a polyvinylidene difluoride membrane (Millipore, Billerica, MA, USA). After blocking with 5 mL 5% skimmed milk for 1 h at room temperature, the primary antibodies were incubated with the membrane overnight at 4 ℃. The next day, the membrane was incubated with the secondary antibody for 2 h at room temperature. Protein blots were analyzed using the enhanced chemiluminescence (ECL) kit (Pierce, Waltham, MA, USA). The intensities of protein bands were quantified using the Image Lab analysis software (National Institutes of Health, Bethesda, MD, USA). The primary antibodies were all purchased from Abcam (Cambridge, MA, USA), including anti-B cell leukemia/lymphoma 2 (anti-Bcl-2; 1/1000; ab32124), anti-Bcl-2 associated X, apoptosis regulator (anti-Bax; 1/1000; ab32503), anti-PAWR (ab92590; 1/10000), and anti-GAPDH (ab8245; 1/5000). Western blot assay was repeated three times.

Lactate dehydrogenase (LDH) assay

Cell death was assessed by quantifying the level of LDH. The release of LDH in the culture supernatant was analyzed using the LDH cytotoxicity assay kit (#C0017; Beyotime, Haimen, China) according to the manufacturer's instructions. In brief, a total of 5×10^3 AC-16 cells were seeded onto 96-well plates. Then, 120 μL of culture supernatant was incubated with 60 μL of LDH test working reagent for 30 min in the dark. The absorbance was detected at the wavelength of 490 nm under a microplate reader (Bio-Rad). LDH assay was repeated three times with six technical repetitions each time.

Bioinformatics analysis

The circHSPG2-miRNA interactions and miR-25-3p-mRNA interactions was established by Starbase database (http://starbase.sysu.edu.cn).

Dual-luciferase reporter assay

The fragment of circHSPG2 or PAWR 3' untranslated region (3'UTR), including the wild-type or mutant binding sites with miR-25-3p, was inserted into pmirGLO plasmid (Promega, Madison, WI, USA) to generate WT/MUT-circHSPG2 and WT/MUT-PAWR 3'UTR. AC-16 cells were seeded onto 24-well plates at 4×10^4 cells/well. The luciferase plasmids (100 ng) were transfected into AC-16 cells with miR-25-3p (50 nM) or miR-NC (50 nM) using Lipofectamine 3000 (Invitrogen). After transfection for 48 h, the luciferase intensities were examined using the commercial dual-luciferase reporter assay system kit (Promega). The intensities of fluorescence were determined using a GloMax 20/20 luminometer (Promega). *Firefly* luciferase intensity was normalized to *Renilla* luciferase activity. Dual-luciferase reporter assay was repeated three times.

RNA immunoprecipitation (RIP) assay

AC-16 cells were plated onto the 6-well plates at 2×10^5 cells/well. AC-16 cells transfected with miR-NC (50 nM) or miR-25-3p (50 nM) were disrupted with the RIP buffer for 5 min on the ice, and then cell lysates were mixed with magnetic beads conjugated with Argonaute 2 (Ago2) antibody (ab186733; 1: 50; Abcam) or immunoglobulin G (IgG) antibody (ab172730; 1: 100; Abcam) for 3 h at 4 ℃. The beads were washed with 500 μL RIP wash buffer twice and were incubated with RIP Immunoprecipitation buffer. The mixture was then centrifuged at 14,000 rpm for 10 min at 4 ℃. RNA was extracted with TRIzol reagent (Invitrogen), and the immune-precipitated RNAs were examined by RT-qPCR. RIP assay was repeated three times.

Statistical analysis

Data were processed by GraphPad Prism 7 software (GraphPad) and were represented as mean ± standard

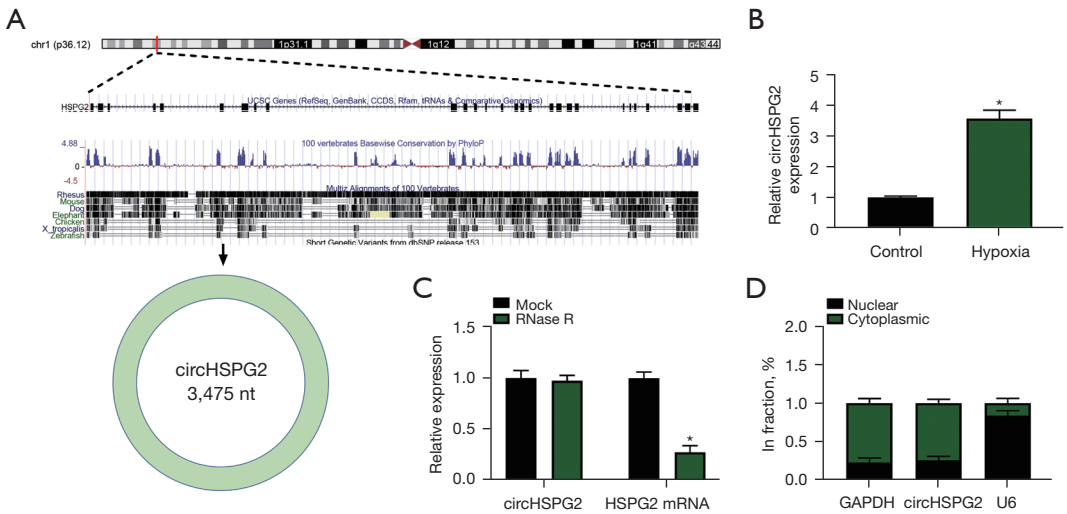

Figure 1 Hypoxia treatment up-regulates circHSPG2 expression in AC-16 cells. (A) The chromosomal localization of circHSPG2 (3475 nt) was shown. (B) The expression of circHSPG2 was determined in AC-16 cells in the control group and hypoxia treatment group by RT-qPCR (Student's *t*-test). (C) The resistance of circHSPG2 to RNase R was analyzed by RT-qPCR, and its linear counterpart HSPG2 was used as the control (two-way ANOVA). (D) The proportion of circHSPG2 in nuclear and cytoplasmic fractions was analyzed using the PARISTM Kit Protein and RNA Isolation system Kit (two-way ANOVA). *, P<0.05. RT-qPCR, reverse transcription-quantitative polymerase chain reaction; ANOVA, analysis of variance.

deviation (SD). The differences were assessed by Student's *t*-test (two groups) or one-way analysis of variance (ANOVA) followed by Tukey's test (three or more groups). P<0.05 was considered statistically significant.

Results

Hypoxia treatment up-regulates circHSPG2 expression in AC-16 cells

The chromosomal localization of circHSPG2 (3475 nt) was shown in *Figure 1A*. We found that circHSPG2 was significantly up-regulated after hypoxia exposure for 24 h in AC-16 cells (*Figure 1B*). CircHSPG2 was resistant to the degradation of RNase R, while RNase R treatment markedly reduced the level of its linear counterpart HSPG2 (*Figure 1C*), suggesting that circHSPG2 was indeed a circular transcript. Before exploring the biological function of circHSPG2, we first analyzed the subcellular localization of circHSPG2. With GAPDH or U6 as cytoplasmic or nuclear indicator, it was found that circHSPG2 was majorly distributed in the cytoplasmic fraction of AC-16 cells (*Figure 1D*), suggesting that circHSPG2 might function in post-transcriptional level.

CircHSPG2 absence alleviates hypoxia-induced dysfunction in AC-16 cells

To explore the biological significance behind the abnormal up-regulation of circHSPG2 in hypoxia-induced AC-16 cells, we performed loss-of-function experiments. Hypoxia-induced up-regulation of circHSPG2 in AC-16 cells was neutralized by si-circHSPG2 (*Figure 2A*). It was observed that hypoxia exposure reduced the viability of AC-16 cells, and this suppressive effect was partly diminished by si-circHSPG2 (*Figure 2B*). Hypoxia treatment suppressed the proliferation of AC-16 cells, evidenced by the reduced percentage of EdU^+ cells and number of colonies (*Figure 2C,2D*). The addition of si-circHSPG2 partly restored the proliferation ability in hypoxia-induced AC-16 cells (*Figure 2C,2D*). Hypoxia-induced the apoptosis of AC-16 cells, which was alleviated by the introduction of si-circHSPG2 (*Figure 2E*). Two apoptosis-associated proteins, including pro-apoptotic protein Bax and anti-apoptotic protein Bcl-2, were measured by Western blot assay. Hypoxia-induced up-regulation of Bax and down-regulation of Bcl-2 were largely reversed by si-circHSPG2 (*Figure 2F*). Combined with the results in *Figure 2E*, these data demonstrated that hypoxia-induced apoptosis in AC-16 cells

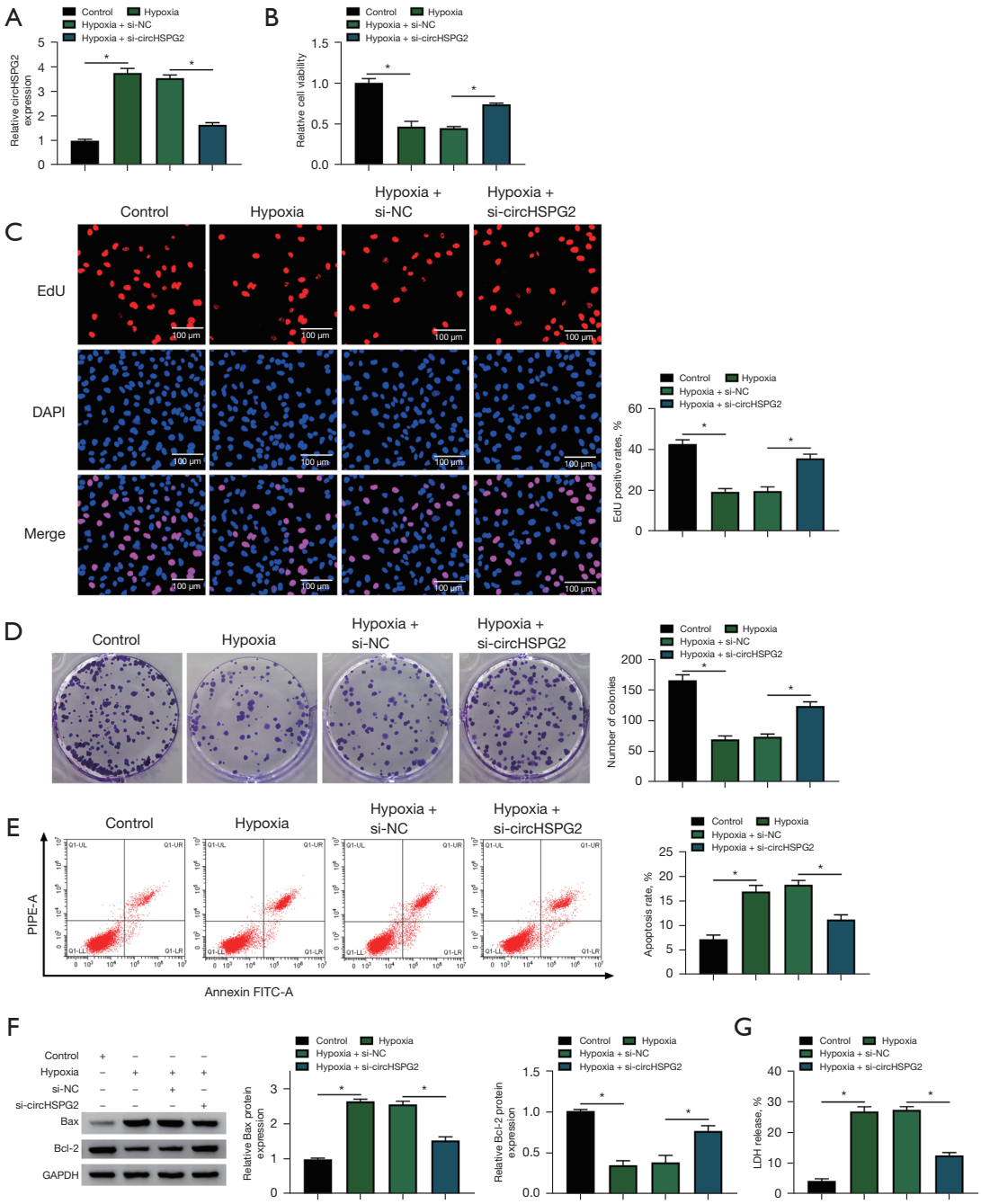

Figure 2 CircHSPG2 absence alleviates hypoxia-induced dysfunction in AC-16 cells. (A-G) AC-16 cells were transfected with si-NC or sicircHSPG2 and then induced by hypoxia for 24 h. (A) The level of circHSPG2 was determined by RT-qPCR (one-way ANOVA). (B) Cell viability in AC-16 cells was examined by MTT assay (one-way ANOVA). (C) EdU assay was conducted to analyze cell proliferation ability (one-way ANOVA). EdU-positive cells were stained red, and nuclei were stained blue by DAPI. (D) Colony formation assay was performed to assess cell proliferation capacity (one-way ANOVA). Cells were stained by crystal violet. (E) FCM analysis was carried out to analyze the apoptosis rate of AC-16 cells (one-way ANOVA). Q1LL: Annexin V–/PI–: viable cells; Q1LR: Annexin V+/PI–: early apoptotic cells; Q1UR: Annexin V+/PI+: late apoptotic cells; Q1UL: Annexin V–/PI+: necrotic cells. (F) Western blot assay was conducted to measure the expression of pro-apoptotic protein Bax and anti-apoptotic protein Bcl-2 in AC-16 cells (one-way ANOVA). (G) LDH assay was performed to analyze cell death (one-way ANOVA). *, P<0.05. RT-qPCR, reverse transcription-quantitative polymerase chain reaction; ANOVA, analysis of variance.

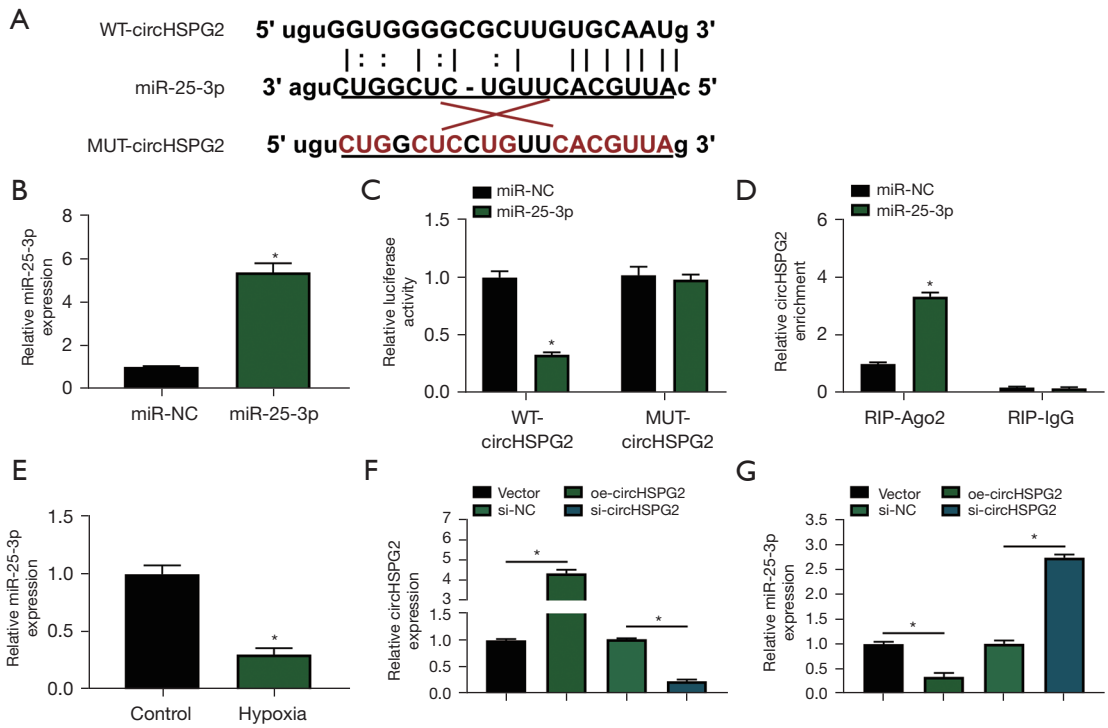

Figure 3 CircHSPG2 negatively regulates miR-25-3p expression by binding to it. (A) The putative binding sequence with circHSPG2 in miR-25-3p was predicted by Starbase database. (B) RT-qPCR was conducted to detect the level of miR-25-3p in AC-16 cells transfected with miR-NC or miR-25-3p (Student's *t*-test). (C) Dual-luciferase reporter assay was conducted to verify the target relationship between circHSPG2 and miR-25-3p (two-way ANOVA). (D) RIP assay was conducted to confirm the target relationship between circHSPG2 and miR-25-3p (two-way ANOVA). (E) The level of miR-25-3p was examined in AC-16 cells upon hypoxia treatment by RT-qPCR (Student's *t*-test). (F and G) The expression of circHSPG2 and miR-25-3p was examined in AC-16 cells transfected with vector, oe-circHSPG2, si-NC, or si-circHSPG2 by RT-qPCR (one-way ANOVA). *, P<0.05. NC, negative control; RT-qPCR, reverse transcription-quantitative polymerase chain reaction; ANOVA, analysis of variance.

was partly dependent on the up-regulation of circHSPG2. LDH assay demonstrated that hypoxia-induced cell death was largely attenuated by the silence of circHSPG2 in AC-16 cells (*Figure 2G*). Taken together, hypoxia-induced dysfunction of AC-16 cells was partly based on the up-regulation of circHSPG2.

CircHSPG2 negatively regulates miR-25-3p expression by binding to it

Bioinformatics software Starbase was utilized to predict the miRNA targets of circHSPG2, and miR-25-3p was predicted as one of the targets of circHSPG2. The putative binding sequence between circHSPG2 and miR-25-3p was shown in *Figure 3A*. RT-qPCR assay confirmed that miR-25-3p mimic (miR-25-3p) was effective in up-regulating miR-25-3p level in AC-16 cells (*Figure 3B*). Dual-luciferase reporter assay and RIP assay were conducted to verify whether circHSPG2 can bind to miR-25-3p. The luciferase activity was significantly reduced in WT-circHSPG2 group with the overexpression of miR-25-3p, while the luciferase activity was unaffected in MUT-circHSPG2 group with the transfection of miR-NC or miR-25-3p (*Figure 3C*), demonstrating that circHSPG2 directly interacted with miR-25-3p. RIP assay revealed that circHSPG2 can bind to exogenous miR-25-3p in RNA-induced silencing complex (RISC) when using Ago2 antibody (*Figure 3D*). Hypoxia treatment reduced the expression of miR-25-3p in AC-16 cells (*Figure 3E*). Then, we analyzed whether circHSPG2 can regulate the expression of miR-25-3p in AC-16 cells. RT-qPCR combined with divergent primers verified the transfection efficiency of circHSPG2 overexpression plasmid (oe-circHSPG2) and si-circHSPG2 in AC-16 cells (*Figure 3F*). CircHSPG2 overexpression notably reduced

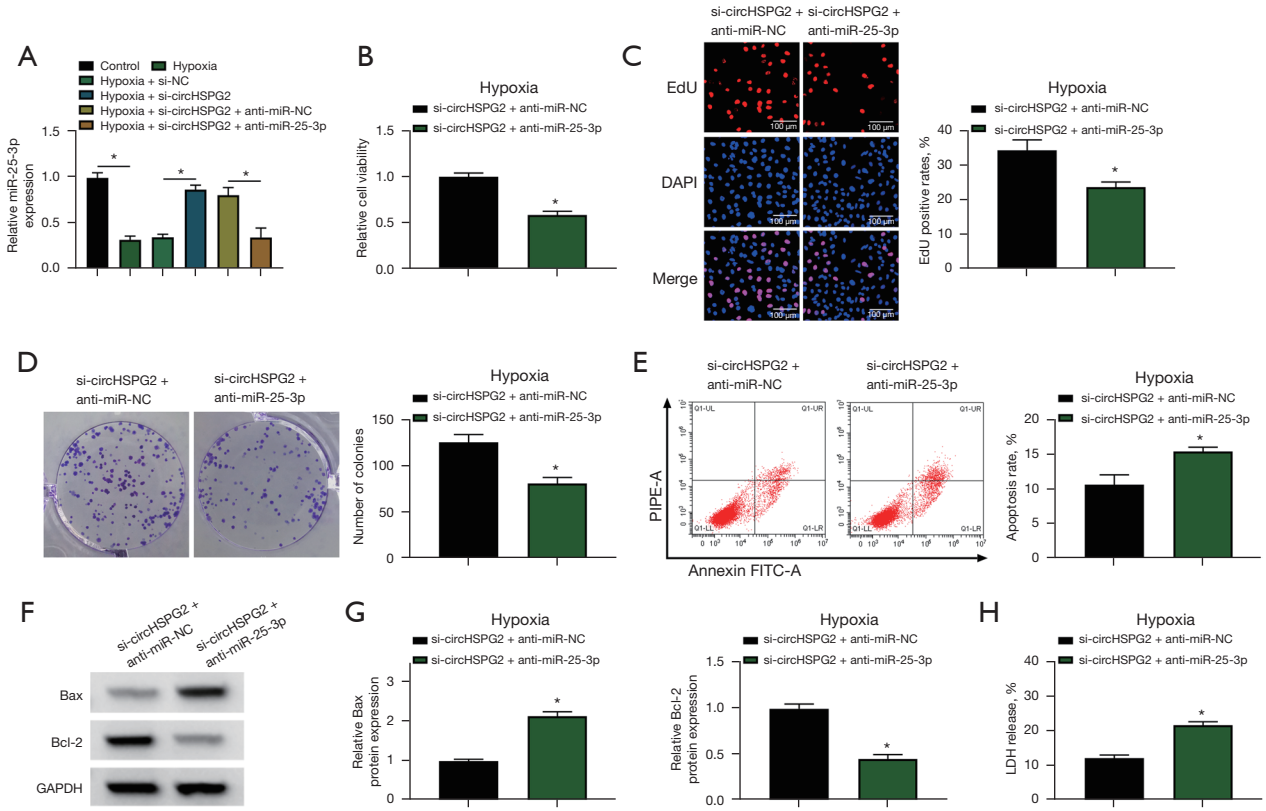

Figure 4 CircHSPG2 silencing-mediated protective effects in hypoxia-induced AC-16 cells are partly overturned by anti-miR-25-3p. (A) AC-16 cells were divided into six groups: Control, hypoxia, hypoxia + si-NC, hypoxia + si-circHSPG2, hypoxia + si-circHSPG2 + antimiR-NC, or hypoxia + si-circHSPG2 + anti-miR-25-3p. The expression of miR-25-3p was examined in AC-16 cells by RT-qPCR (one-way ANOVA). (B-H) AC-16 cells were divided into two groups: hypoxia + si-circHSPG2 + anti-miR-NC and hypoxia + si-circHSPG2 + anti-miR-25-3p. (B) Cell viability was analyzed by MTT assay (Student's *t*-test). (C,D) EdU assay (EdU-positive cells were stained red, and nuclei were stained blue by DAPI) and colony formation assay (cells were stained by crystal violet) were conducted to analyze the proliferation ability of AC-16 cells (Student's *t*-test). (E) The apoptosis rate of AC-16 cells was examined by FCM analysis (Student's *t*-test). (F and G) The protein levels of Bax and Bcl-2 were examined by Western blot assay (Student's *t*-test). (H) Cell death was analyzed by LDH assay (Student's *t*-test). *, P<0.05. RT-qPCR, reverse transcription-quantitative polymerase chain reaction; ANOVA, analysis of variance.

the expression of miR-25-3p, and circHSPG2 absence markedly up-regulated miR-25-3p level in AC-16 cells (*Figure 3G*). These results together demonstrated that miR-25-3p was a target of circHSPG2, and it was negatively regulated by circHSPG2 in AC-16 cells.

CircHSPG2 silencing-mediated protective effects in hypoxia-induced AC-16 cells are partly overturned by anti-miR-25-3p

Considering that circHSPG2 absence up-regulated the expression of miR-25-3p, we co-transfected hypoxia-induced AC-16 cells with si-circHSPG2 and anti-miR-25-3p to explore whether circHSPG2 silencing-induced effects were partly dependent on the up-regulation of miR-25-3p. The addition of anti-miR-25-3p reduced the expression of miR-25-3p in AC-16 cells (*Figure 4A*). Cell viability was decreased by the addition of anti-miR-25-3p in AC-16 cells (*Figure 4B*). The introduction of anti-miR-25-3p suppressed the proliferation of AC-16 cells (*Figure 4C,4D*). The addition of anti-miR-25-3p triggered the apoptosis of AC-16 cells (*Figure 4E*). The protein expression of Bax was up-regulated while the protein level of Bcl-2 was reduced by silencing miR-25-3p (*Figure 4F,4G*). The addition of anti-miR-25-3p induced cell death (*Figure 4H*). Overall, circHSPG2 silencing-mediated protective effects in

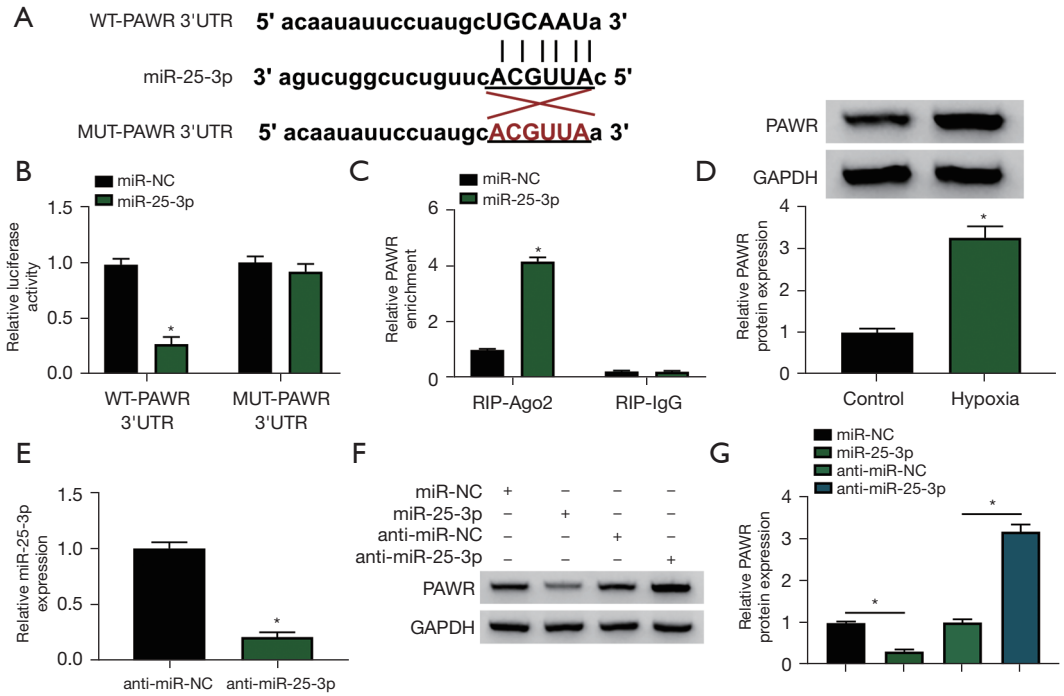

Figure 5 miR-25-3p binds to the 3'UTR of PAWR in AC-16 cells. (A) The putative binding sites between miR-25-3p and PAWR 3'UTR predicted by Starbase database were shown. (B and C) The associated relationship between miR-25-3p and PAWR was validated by dual-luciferase reporter assay and RIP assay (two-way ANOVA). (D) Western blot assay was conducted to measure the protein level of PAWR in AC-16 cells exposed to hypoxia for 24 h (Student's *t*-test). (E) The transfection efficiency of anti-miR-25-3p was determined in AC-16 cells by RT-qPCR (Student's *t*-test). (F and G) The effect of miR-25-3p overexpression or knockdown on the protein expression of PAWR in AC-16 cells was assessed by Western blot assay (one-way ANOVA). *, P<0.05. NC, negative control; RT-qPCR, reverse transcription-quantitative polymerase chain reaction; PAWR, pro-apoptotic WT1 regulator; ANOVA, analysis of variance.

hypoxia-induced AC-16 cells were largely based on the up-regulation of miR-25-3p.

miR-25-3p binds to the 3'UTR of PAWR in AC-16 cells

The possible mRNA targets of miR-25-3p were predicted by Starbase database, and the putative binding sequence between miR-25-3p and *PAWR* was shown in *Figure 5A*. The overexpression of miR-25-3p significantly reduced the luciferase activity of WT-PAWR 3'UTR rather than MUT-PAWR 3'UTR (*Figure 5B*), suggesting that miR-25-3p directly interacted with the 3'UTR of *PAWR*. RIP assay revealed that there was spatial interaction between miR-25-3p and *PAWR* in RISC (*Figure 5C*). The expression of PAWR protein was markedly up-regulated in AC-16 cells upon hypoxia treatment (*Figure 5D*) and si-PAWR introduction repressed PAWR protein levels in AC-16 cells with hypoxia treatment (Figure S1A). Also, PAWR silencing weakened hypoxia-mediated effects on AC-16 cell proliferation, apoptosis, and cytotoxicity (Figure S1B-S1G). High transfection efficiency of anti-miR-25-3p was verified by RT-qPCR in AC-16 cells (*Figure 5E*). miR-25-3p overexpression reduced the protein expression of PAWR, and miR-25-3p knockdown up-regulated the level of PAWR protein in AC-16 cells (*Figure 5F,5G*). Taken together, miR-25-3p negatively regulated *PAWR* expression by interacting with its 3'UTR in AC-16 cells.

miR-25-3p overexpression protects AC-16 cells from hypoxia-induced dysfunction partly by down-regulating PAWR

Rescue experiments were conducted to analyze whether miR-25-3p regulated the biological phenotypes of AC-16 cells by targeting *PAWR*. miR-25-3p overexpression reduced the protein expression of PAWR, and the protein

level of PAWR was largely recovered by the addition of PAWR plasmid (*Figure 6A*). miR-25-3p overexpression protected AC-16 cells from hypoxia-induced dysfunction in AC-16 cells (*Figure 6B-6H*). Furthermore, the addition of PAWR plasmid reduced the viability and suppressed the proliferation of AC-16 cells (*Figure 6B-6D*). PAWR overexpression also induced the apoptosis of AC-16 cells (*Figure 6E*). The protein level of Bax was up-regulated while the protein level of Bcl-2 was decreased by the introduction of PAWR plasmid (*Figure 6F,6G*). LDH assay displayed that cell death was induced by the addition of PAWR plasmid (*Figure 6H*). Collectively, miR-25-3p exerted a protective role in hypoxia-induced AC-16 cells partly by down-regulating PAWR.

CircHSPG2 acts as a positive regulator of PAWR by sequestering miR-25-3p in AC-16 cells

CircHSPG2 absence reduced the protein expression of PAWR, and the protein level of PAWR was largely rescued by the addition of anti-miR-25-3p in AC-16 cells (*Figure 7A*). CircHSPG2 overexpression increased the protein expression of PAWR, and addition of miR-25-3p decreased the protein level of PAWR in AC-16 cells (*Figure 7B*). These results suggested that circHSPG2 positively regulated *PAWR* expression by sponging miR-25-3p in AC-16 cells.

Discussion

Due to the high stability, abundant expression, and tissue-specific expression pattern, circRNAs are considered as promising bio-markers for human diseases (20). Nevertheless, the biological roles of circRNAs in cardiac pathophysiology remain largely unknown. Several articles reported that circRNAs are dysregulated in multiple cardiovascular diseases. For instance, circ_000203 is reported to be up-regulated in mouse model and cell model of cardiac hypertrophy, and circ_000203 facilitates cardiac hypertrophy progression by targeting miR-26b-5p/miR-140-3p-*Gata4* axis (21). CircTLK1 is reported to be up-regulated in myocardial ischemia/reperfusion injury mouse model, and it aggravates ischemia/reperfusion injury through mediating miR-214/*RIPK1* signaling (22). As for circHSPG2, previous studies found that circHSPG2 absence exerts a protective role in cardiomyocytes upon the stimulation of hypoxia or oxygen-glucose deprivation (9,23,24). We found that hypoxia exposure enhanced the expression of circHSPG2 in cardiomyocytes. Hypoxia treatment inhibited the viability and proliferation and induced the apoptosis of cardiomyocytes, and circHSPG2 silencing using si-circHSPG2 attenuated hypoxia-induced dysfunction in cardiomyocytes, suggesting that the up-regulation of circHSPG2 was important for hypoxia-induced dysfunction in cardiomyocytes. A previous report showed that hyperoxia gradually increases cellular inflammation and cytotoxicity (25), and whether hyperoxia affects the level of circHSPG2 in cardiomyocytes can be further explored in the future.

Accumulating evidence have verified that circRNAs can sequester miRNAs to regulate the expression and biological roles of miRNAs (11,26). Through bioinformatics analysis using Starbase software and experimental verification, the associated relationship between circHSPG2 and miR-25-3p was validated. Hypoxia stimulation reduced the level of miR-25-3p, and miR-25-3p was reversely modulated by circHSPG2 in AC-16 cells. miR-25-3p is identified to be a pro-tumor factor in multiple cancers (27-30). As for hypoxia-induced myocardial damage, Qin *et al*. found that miR-25 abundance is reduced in hypoxia-induced cardiomyocytes, and it facilitates the proliferation and migration capacities and reduces the apoptotic rate of cardiomyocytes (17). Two previous studies reported that miR-25 protects cardiomyocytes from oxidation or sepsis-induced injury by targeting mitochondrial calcium uniporter (15) or PTEN (16), respectively. Consistently, we found that miR-25-3p overexpression largely restored the viability and proliferation and suppressed the apoptosis of hypoxia-treated AC-16 cells. To investigate whether circHSPG2 functioned by targeting miR-25-3p in hypoxia-induced AC-16 cells, rescue experiments were implemented. The results presented that circHSPG2 absence protected AC-16 cells from hypoxia-induced dysfunction partly by up-regulating miR-25-3p, which further demonstrated the protective role of miR-25-3p in AC-16 cells upon hypoxia stimulation.

The interaction between miR-25-3p and PAWR was identified in AC-16 cells. It was observed that hypoxia stimulation up-regulated the protein expression of PAWR in AC-16 cells. PAWR was reversely modulated by miR-25-3p in AC-16 cells. Previous articles reported that PAWR acts as an anti-tumor factor in multiple cancers by inhibiting cell proliferation and inducing cell apoptosis (31-33). Moreover, it is reported that circ_0068655 facilitates the apoptosis of cardiomyocytes by binding to miR-498 to up-regulate the expression of *PAWR* (18). We found that miR-25-3p

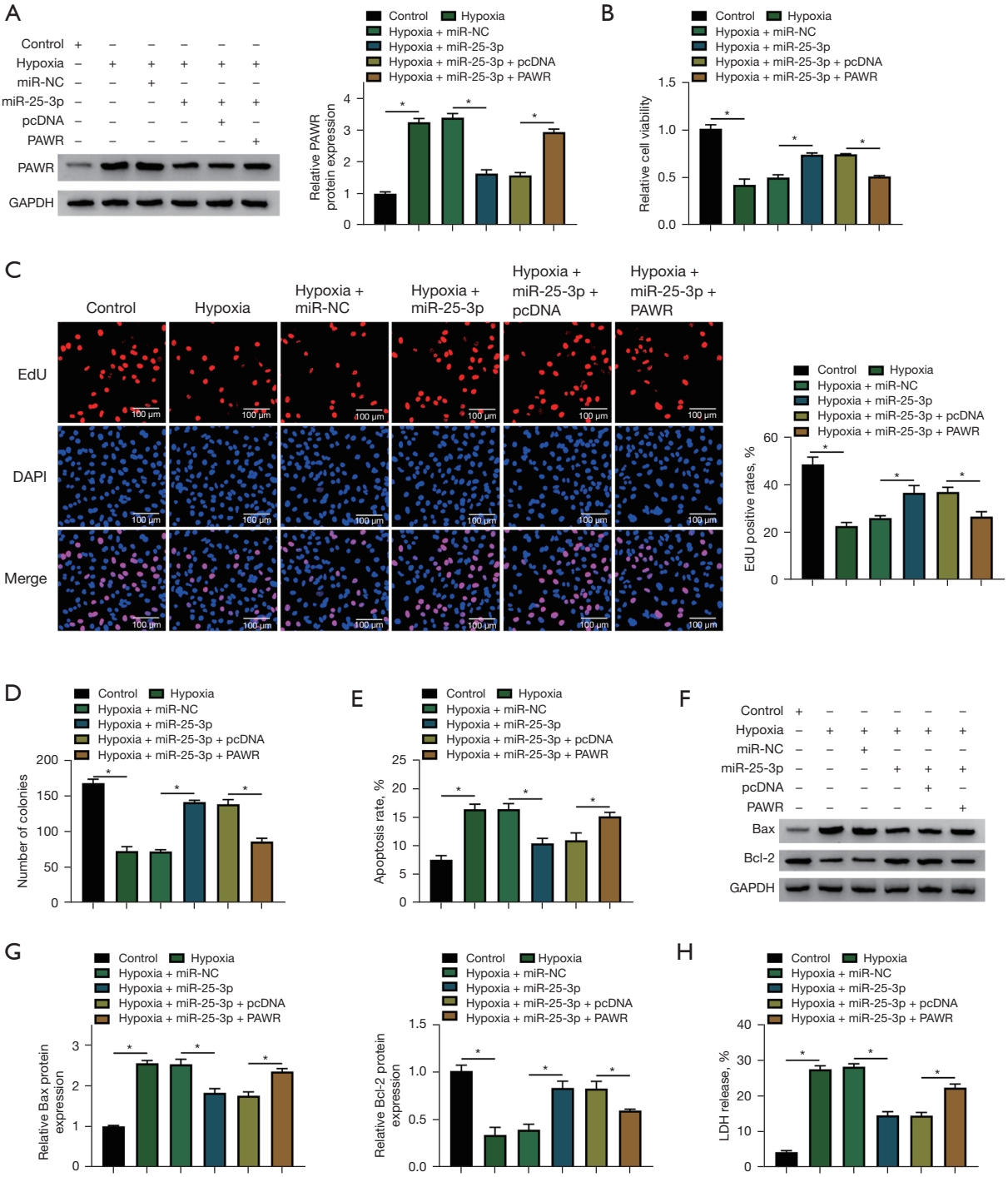

Figure 6 miR-25-3p overexpression protects AC-16 cells from hypoxia-induced dysfunction partly by down-regulating PAWR. (A-H) AC-16 cells were transfected with miR-25-3p alone or together with PAWR plasmid and then exposed to hypoxia. (A) The protein level of PAWR in AC-16 cells was examined by Western blot assay (one-way ANOVA). (B) MTT assay was performed to determine the viability of transfected AC-16 cells (one-way ANOVA). (C and D) EdU assay (EdU-positive cells were stained red, and nuclei were stained blue by DAPI) and colony formation assay (cells were stained by crystal violet) were implemented to analyze the proliferation of AC-16 cells (one-way ANOVA). (E) FCM analysis was used to evaluate the apoptosis of AC-16 cells (one-way ANOVA). (F,G) The protein levels of Bax and Bcl-2 were examined in AC-16 cells by Western blot assay (one-way ANOVA). (H) LDH assay was conducted to analyze cell death (one-way ANOVA). *, P<0.05. PAWR, pro-apoptotic WT1 regulator; ANOVA, analysis of variance.

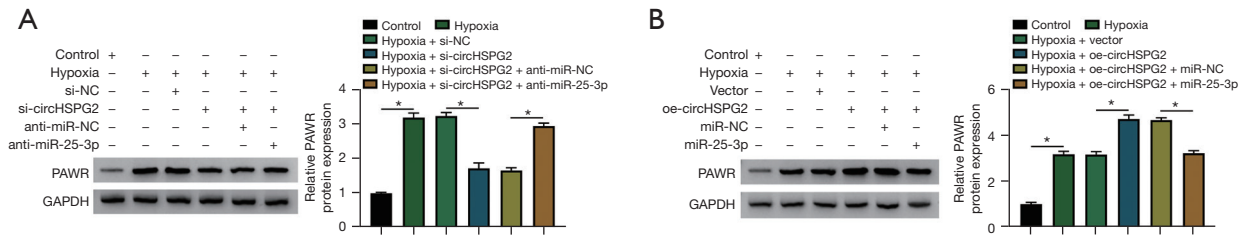

Figure 7 CircHSPG2 acts as a positive regulator of PAWR by sequestering miR-25-3p in AC-16 cells. (A) Western blot assay was conducted to measure the protein level of PAWR in AC-16 cells in the following six groups: Control, hypoxia, hypoxia + si-NC, hypoxia + si-circHSPG2, hypoxia + si-circHSPG2 + anti-miR-NC, or hypoxia + si-circHSPG2 + anti-miR-25-3p (one-way ANOVA). (B) The protein level of PAWR was determined in AC-16 cells in the following six groups by Western blot assay: Control, hypoxia, hypoxia + vector, hypoxia + oe-circHSPG2, hypoxia + oe-circHSPG2 + miR-NC, or hypoxia + oe-circHSPG2 + miR-25-3p (one-way ANOVA). *, P<0.05. PAWR, pro-apoptotic WT1 regulator; ANOVA, analysis of variance; NC, negative control.

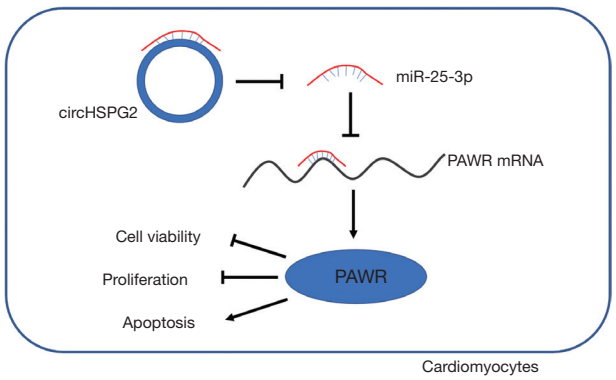

Figure 8 CircHSPG2 contributes to hypoxia-induced dysfunction in AC-16 cells by targeting miR-25-3p/PAWR axis. PAWR, pro-apoptotic WT1 regulator.

overexpression-mediated protective effects in hypoxia-induced AC-16 cells were largely reversed by the addition of PAWR plasmid, indicating that miR-25-3p protected AC-16 cells from hypoxia-induced dysfunction partly by down-regulating *PAWR*. Finally, it was found that circHSPG2 acted as a positive regulator of *PAWR* by acting as miR-25-3p sponge in AC-16 cells. *FBXW7* is reported as another target of miR-25 (34), and whether *FBXW7* is regulated by the circHSPG2/miR-25-3p axis can be explored in the future.

In summary, the data in this study together presented that circHSPG2 absence protected AC-16 cells from hypoxia-induced injury through mediating miR-25-3p/*PAWR* axis (*Figure 8*). Our results suggested that circHSPG2 knockdown might be a promising therapeutic strategy to alleviate hypoxia-induced myocardial damage. In future, animal experiment is needed to analyze the effect, side effect, and specificity of circHSPG2 knockdown therapy in myocardial infarction treatment.

Acknowledgments

Thanks for all participants involved in this study.
Funding: This study was supported by Research Project of health industry in Hainan Province (No. 20A200060).

Footnote

Data Sharing Statement: Available at https://cdt.amegroups.com/article/view/10.21037/cdt-22-197/dss

Peer Review File: Available at https://cdt.amegroups.com/article/view/10.21037/cdt-22-197/prf

Conflicts of Interest: All authors have completed the ICMJE uniform disclosure form (available at https://cdt.amegroups.com/article/view/10.21037/cdt-22-197/coif). The authors have no conflicts of interest to declare.

Ethical Statement: The authors are accountable for all aspects of the work in ensuring that questions related to the accuracy or integrity of any part of the work are appropriately investigated and resolved. The study was conducted in accordance with the Declaration of Helsinki (as revised in 2013).

References

1. George TA, Hsu CC, Meeson A, et al. Nanocarrier-Based Targeted Therapies for Myocardial Infarction. Pharmaceutics 2022;14:930.
2. Frangogiannis NG. Pathophysiology of Myocardial Infarction. Compr Physiol 2015;5:1841-75.
3. He L, Chen X. Cardiomyocyte Induction and Regeneration for Myocardial Infarction Treatment: Cell Sources and Administration Strategies. Adv Healthc Mater 2020;9:e2001175.
4. Bahit MC, Kochar A, Granger CB. Post-Myocardial Infarction Heart Failure. JACC Heart Fail 2018;6:179-86.
5. Jenča D, Melenovský V, Stehlik J, et al. Heart failure after myocardial infarction: incidence and predictors. ESC Heart Fail 2021;8:222-37.
6. Li M, Ding W, Sun T, et al. Biogenesis of circular RNAs and their roles in cardiovascular development and pathology. FEBS J 2018;285:220-32.
7. Fan X, Weng X, Zhao Y, et al. Circular RNAs in Cardiovascular Disease: An Overview. Biomed Res Int 2017;2017:5135781.
8. Dang RY, Liu FL, Li Y. Circular RNA hsa_circ_0010729 regulates vascular endothelial cell proliferation and apoptosis by targeting the miR-186/HIF-1α axis. Biochem Biophys Res Commun 2017;490:104-10.
9. Lei D, Wang Y, Zhang L, et al. Circ_0010729 regulates hypoxia-induced cardiomyocyte injuries by activating TRAF5 via sponging miR-27a-3p. Life Sci 2020;262:118511.
10. Zhang J, Gao C, Zhang J, et al. Circ_0010729 knockdown protects cardiomyocytes against hypoxic dysfunction via miR-370-3p/TRAF6 axis. EXCLI J 2020;19:1520-32.
11. Hansen TB, Jensen TI, Clausen BH, et al. Natural RNA circles function as efficient microRNA sponges. Nature 2013;495:384-8.
12. Jiao M, You HZ, Yang XY, et al. Circulating microRNA signature for the diagnosis of childhood dilated cardiomyopathy. Sci Rep 2018;8:724.
13. Batkai S, Bär C, Thum T. MicroRNAs in right ventricular remodelling. Cardiovasc Res 2017;113:1433-40.
14. Wu T, Chen Y, Du Y, et al. Serum Exosomal MiR-92b-5p as a Potential Biomarker for Acute Heart Failure Caused by Dilated Cardiomyopathy. Cell Physiol Biochem 2018;46:1939-50.
15. Pan L, Huang BJ, Ma XE, et al. MiR-25 protects cardiomyocytes against oxidative damage by targeting the mitochondrial calcium uniporter. Int J Mol Sci 2015;16:5420-33.
16. Yao Y, Sun F, Lei M. miR-25 inhibits sepsis-induced cardiomyocyte apoptosis by targetting PTEN. Biosci Rep 2018;38:BSR20171511.
17. Qin X, Gao S, Yang Y, et al. microRNA-25 promotes cardiomyocytes proliferation and migration via targeting Bim. J Cell Physiol 2019;234:22103-15.
18. Chai Q, Zheng M, Wang L, et al. Circ_0068655 Promotes Cardiomyocyte Apoptosis via miR-498/PAWR Axis. Tissue Eng Regen Med 2020;17:659-70.
19. Davidson MM, Nesti C, Palenzuela L, et al. Novel cell lines derived from adult human ventricular cardiomyocytes. J Mol Cell Cardiol 2005;39:133-47.
20. Zhang Z, Yang T, Xiao J. Circular RNAs: Promising Biomarkers for Human Diseases. EBioMedicine 2018;34:267-74.
21. Li H, Xu JD, Fang XH, et al. Circular RNA circRNA_000203 aggravates cardiac hypertrophy via suppressing miR-26b-5p and miR-140-3p binding to Gata4. Cardiovasc Res 2020;116:1323-34.
22. Song YF, Zhao L, Wang BC, et al. The circular RNA TLK1 exacerbates myocardial ischemia/reperfusion injury via targeting miR-214/RIPK1 through TNF signaling pathway. Free Radic Biol Med 2020;155:69-80.
23. Jin Q, Chen Y. Silencing circular RNA circ_0010729 protects human cardiomyocytes from oxygen-glucose deprivation-induced injury by up-regulating microRNA-145-5p. Mol Cell Biochem 2019;462:185-94.
24. Wang Y, Wu C, Zhang Y, et al. Screening for differentially expressed circRNA between Kashin-Beck disease and osteoarthritis patients based on circRNA chips. Clin Chim Acta 2020;501:92-101.
25. Hafner C, Wu J, Tiboldi A, et al. Hyperoxia Induces Inflammation and Cytotoxicity in Human Adult Cardiac Myocytes. Shock 2017;47:436-44.
26. Kulcheski FR, Christoff AP, Margis R. Circular RNAs are miRNA sponges and can be used as a new class of biomarker. J Biotechnol 2016;238:42-51.
27. Chen H, Pan H, Qian Y, et al. MiR-25-3p promotes the proliferation of triple negative breast cancer by targeting

BTG2. Mol Cancer 2018;17:4.
28. Ning L, Zhang M, Zhu Q, et al. miR-25-3p inhibition impairs tumorigenesis and invasion in gastric cancer cells in vitro and in vivo. Bioengineered 2020;11:81-90.
29. Wan W, Wan W, Long Y, et al. MiR-25-3p promotes malignant phenotypes of retinoblastoma by regulating PTEN/Akt pathway. Biomed Pharmacother 2019;118:109111.
30. Rao HC, Wu ZK, Wei SD, et al. MiR-25-3p Serves as an Oncogenic MicroRNA by Downregulating the Expression of Merlin in Osteosarcoma. Cancer Manag Res 2020;12:8989-9001.
31. Song R, Li Y, Hao W, et al. Circular RNA MTO1 inhibits gastric cancer progression by elevating PAWR via sponging miR-199a-3p. Cell Cycle 2020;19:3127-39.
32. Yang K, Shen J, Chen SW, et al. Upregulation of PAWR by small activating RNAs induces cell apoptosis in human prostate cancer cells. Oncol Rep 2016;35:2487-93.
33. Pereira MC, de Bessa-Garcia SA, Burikhanov R, et al. Prostate apoptosis response-4 is involved in the apoptosis response to docetaxel in MCF-7 breast cancer cells. Int J Oncol 2013;43:531-8.
34. Wang B, Xu M, Li M, et al. miR-25 Promotes Cardiomyocyte Proliferation by Targeting FBXW7. Mol Ther Nucleic Acids 2020;19:1299-308.

Cite this article as: Zhao Y, Wang S, Liu S, Yan Q, Li Y, Liu Y. CircHSPG2 absence weakens hypoxia-induced dysfunction in cardiomyocytes by targeting the miR-25-3p/PAWR axis. Cardiovasc Diagn Ther 2022;12(5):589-602. doi: 10.21037/cdt-22-197

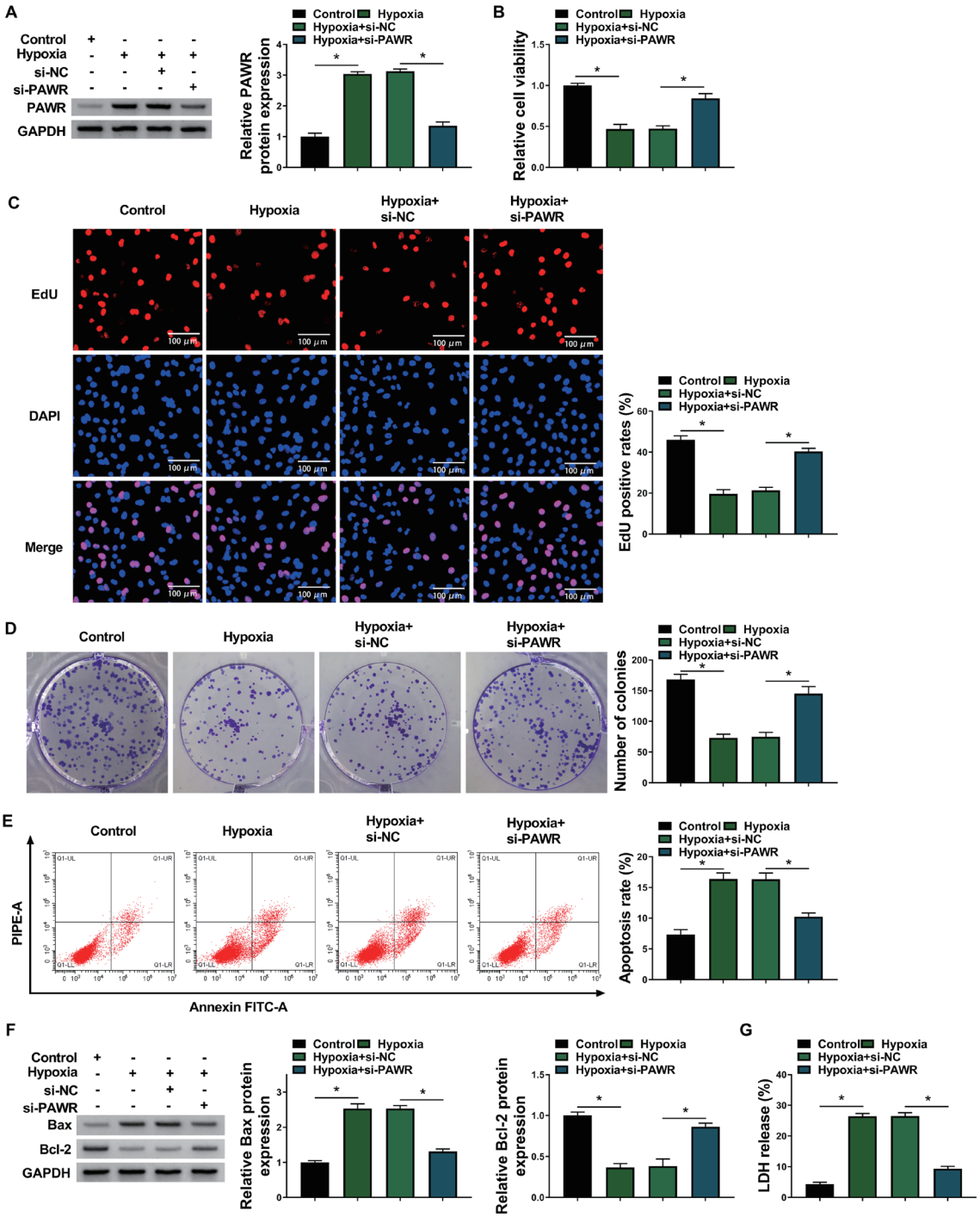

Figure S1 PAWR silencing alleviates hypoxia-induced dysfunction in AC-16 cells. (A-G) AC-16 cells were transfected with si-NC or si-PAWR and then induced by hypoxia for 24 h. (A) PAWR protein levels were determined by RT-qPCR (one-way ANOVA). (B) Cell viability was examined by MTT assay (one-way ANOVA). (C) EdU assay analyzed cell proliferation ability (one-way ANOVA). (D) Colony formation assay assessed cell proliferation capacity (one-way ANOVA). (E) FCM analysis analyzed the apoptosis rate of AC-16 cells (one-way ANOVA). Q1LL: Annexin V-/PI-: viable cells; Q1LR: Annexin V+/PI-: early apoptotic cells; Q1UR: Annexin V+/PI+: late apoptotic cells; Q1UL: Annexin V-/PI+: necrotic cells. (F) Western blot assay detected Bax and Bcl-2 protein levels in AC-16 cells (one-way ANOVA). (G) LDH assay was performed to analyze cell death (one-way ANOVA). *, P<0.05. PAWR, pro-apoptotic WT1 regulator; RT-qPCR, reverse transcription-quantitative polymerase chain reaction.

https://dx.doi.org/10.21037/cdt-22-197